



## Brief paper

Calculating switching times for the time-optimal control of single-input, single-output second-order systems<sup>☆</sup>Zhaolong Shen<sup>a</sup>, Peng Huang<sup>b</sup>, Sean B. Andersson<sup>b,1</sup><sup>a</sup> Department of Bioengineering, University of Maryland, College Park, MD, 20742, USA<sup>b</sup> Department of Mechanical Engineering and Division of Systems Engineering, Boston University, Boston, MA, 02215, USA

## ARTICLE INFO

## Article history:

Received 16 June 2011

Received in revised form

1 November 2012

Accepted 4 December 2012

Available online 16 March 2013

## Keywords:

Time-optimal control

Switching times

Bang–bang control

## ABSTRACT

In this paper, we consider the time-optimal control of a single-input, single-output second-order system with bounded input and describe a method for calculating the number of switches and the switching times to drive the system from any initial state to a target state in a particular class. A pair of affine mappings are derived that transform the original system into one where the switching curve becomes a collection of similar sections of a logarithmic spiral. In this coordinate system, the number of switches and the times of those switches are calculated and a feedback control law is synthesized.

© 2013 Elsevier Ltd. All rights reserved.

## 1. Introduction

The Pontryagin Maximum Principle (PMP) (Pontryagin, Boltyanskii, Gamkrelidze, & Mishchenko, 1962) shows that a time-optimal solution for steering a linear system with bounded inputs between two states can be achieved by a series of switches between the extremes of the control. Time-optimal methods have been applied successfully in, for example, the control of hard disk drives (Iamratanakul, Jordan, Leang, & Devasia, 2008; La-orpacharapan & Pao, 2004; McCormick & Horowitz, 1991) and of quantum spin systems (Khaneja, Brockett, & Glaser, 2001; Khaneja, Reiss, Kehlet, Schulte-Herbrüggen, & Glaser, 2005).

Current schemes do not easily yield the number of switches or the switching times needed to effect the transfer. While this information can be calculated through simulation, a simpler solution would be useful when doing online optimization of the path to move through a collection of target states in minimum time by using the transition times between any two targets to formulate a traveling salesman problem. Two examples of this are moving between measurement locations when tracking multiple but widely

separated objects using a single mobile sensor (Shen & Andersson, 2011) or when moving the tip of an atomic force microscope through a random selection of measurement locations to reduce the total number of measurements needed to produce an image (Andersson & Pao, 2012).

In this paper, we consider a second-order, single-input, single-output (SISO), linear time-invariant (LTI) system and develop a pair of affine maps which convert the system into a standard form. In this form, the switching curve is given by a collection of similar logarithmic spirals and the boundaries between regions of constant control by another such collection. For equilibrium points for which there is sufficient control authority to hold the system at the target state, we determine the number of switches, the switching times, and synthesize a feedback controller. The method allows for control bounds that do not include the zero input in their range.

## 2. Problem formulation

Consider a strictly proper, second-order, LTI, SISO system with transfer function given by

$$\frac{Y(s)}{U(s)} = \frac{b_1 s + b_2}{s^2 + a_1 s + a_2}. \quad (1)$$

The input is assumed to be bounded,  $u \in [u_{\min}, u_{\max}] \subset \mathbb{R}$ . Note that  $u_{\min}$  and  $u_{\max}$  are allowed to have the same sign and therefore 0 does not need to be in the set.

We express the system in observable canonical form

$$\dot{x} = Ax + Bu, \quad (2)$$

<sup>☆</sup> This material is based in part upon work supported by the NSF grants DBI-0649823 and CMMI-0845742. The material in this paper was not presented at any conference. This paper was recommended for publication in revised form by Associate Editor Fen Wu under the direction of Editor Roberto Tempo.

E-mail addresses: [zhaolong.shen@gmail.com](mailto:zhaolong.shen@gmail.com) (Z. Shen), [huangp09@bu.edu](mailto:huangp09@bu.edu) (P. Huang), [sanderss@bu.edu](mailto:sanderss@bu.edu) (S.B. Andersson).

<sup>1</sup> Tel.: +1 6173534949; fax: +1 6173535866.

where

$$A = \begin{bmatrix} 0 & 1 \\ -a_2 & -a_1 \end{bmatrix}, \quad B = \begin{bmatrix} b_1 \\ b_2 - a_1 b_1 \end{bmatrix}.$$

The eigenvalues of  $A$  are

$$\lambda_{1,2} = -\frac{a_1}{2} \pm i\omega, \quad \omega = \frac{\sqrt{4a_2 - a_1^2}}{2}. \quad (3)$$

We assume

$$a_1 \neq 0, \quad 4a_2 > a_1^2, \quad (4)$$

such that the eigenvalues are neither pure real nor pure imaginary. We consider the following problem.

**Problem 1.** Given (2) satisfying (4) with control bounds  $u_{\min}, u_{\max}$ , an initial state  $x_o$ , and a target state  $x_r$ , find a control law to steer the system from  $x_o$  to  $x_r$  in minimum time.

Target states can be categorized into three types.

**Definition 1.** A target state  $x_r$  is called a

- *holdable equilibrium* if  $\exists u_o \in (u_{\min}, u_{\max})$  such that  $Ax_r + Bu_o = 0$ .
- *non-holdable equilibrium* if  $\exists u_o \in (-\infty, u_{\min}) \cup (u_{\max}, \infty)$  such that  $Ax_r + Bu_o = 0$ .
- *non-equilibrium* if  $Ax_r + Bu_o \neq 0 \forall u_o \in \mathbb{R}$ .

The holdable equilibrium target states are those for which there is sufficient control authority to hold the system fixed at the target point after the transition while the non-holdable equilibrium states are those for which the system could be held fixed if there was additional control authority. The combined set of equilibrium target points lie on the line defined by

$$X_{eq} = \{x \in \mathbb{R}^2 | x = -A^{-1}Bu_o, u_o \in \mathbb{R}\}.$$

Points off the line are non-equilibrium points.

### 2.1. PMP and the switching curve

Applying the PMP to Problem 1 yields the bang–bang law

$$u^*(t) = \begin{cases} u_{\min}, & \text{if } \psi^T(t)B < 0, \\ u_{\max}, & \text{if } \psi^T(t)B > 0, \end{cases} \quad (5)$$

with  $u^* \in [u_{\min}, u_{\max}]$  arbitrary for  $\psi^T(t)B = 0$ . Here  $\psi(t) \in \mathbb{R}^2$  is the costate vector with dynamics

$$\dot{\psi}(t) = -A^T \psi(t). \quad (6)$$

Under the optimal control law, a switch occurs when  $\psi^T(t)B = 0$ . In addition, at the final time the following boundary condition is satisfied:

$$\psi^T(t_f)(Ax(t_f) + Bu^*(t_f)) \geq 0. \quad (7)$$

The standard solution to this problem is as follows (see, e.g. Pontryagin et al. (1962)). Define a line segment in the costate space by the two points  $v_{1,2} = Bu_{\min, \max}$  (see Fig. 1). The costate space is divided into two half-planes by the line passing through the origin and perpendicular to the line segment  $v_1-v_2$ . Under the switching law (5), the optimal control takes the value  $u_{\min}$  ( $u_{\max}$ ) if the costate is in the half-plane containing  $v_1$  ( $v_2$ ). Unlike our approach, this assumes that zero is an allowed control input.

The costate rotates at the rate  $\omega$  given in (3). As a result, along an optimal trajectory the control is constant for no longer than  $\pi/\omega$  units of time. The time interval before the first switch and the interval between the final switch and arrival at the target state are

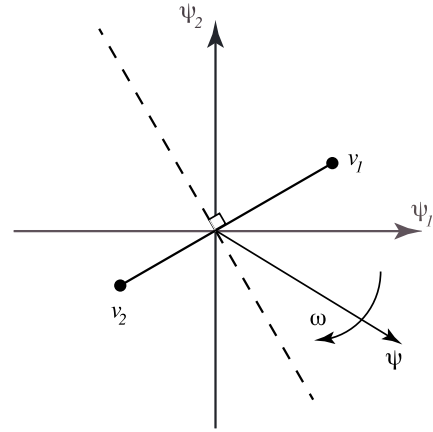


**Fig. 1.** The switching condition divides the costate space into two half-planes with the optimal control being  $u_{\min}$  ( $u_{\max}$ ) when  $\psi$  is in the half-plane containing  $v_1$  ( $v_2$ ).

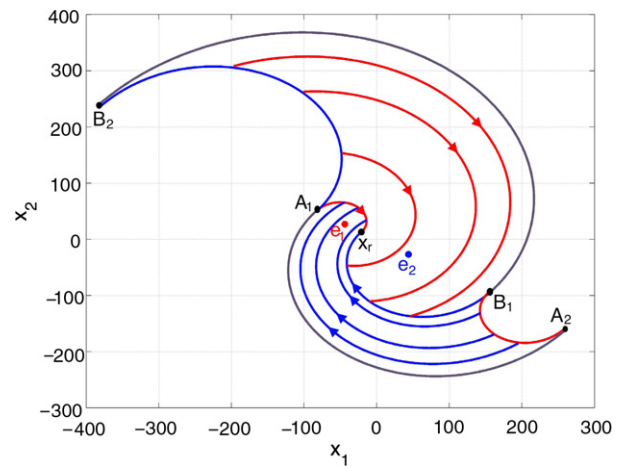


**Fig. 2.** The switching curve and optimal trajectories in state space for a target point  $x_r$ . Evolving backwards in time from  $x_r$  under  $u_{\min}$  ( $A_1x_r$ , red) or  $u_{\max}$  ( $B_1x_r$ , blue) produces two final trajectories. Rotating and scaling these as described in Section 2.1 produces the switching curve (alternating red–blue). (For interpretation of the references to colour in this figure legend, the reader is referred to the web version of this article.)

determined by the initial and final values of the costate (and therefore by the initial and final values of the state) while all intermediate intervals last exactly  $\pi/\omega$  units of time.

The switching condition similarly divides the state space as follows. Define the vectors  $e_1$  and  $e_2$  according to

$$e_{1,2} = -A^{-1}Bu_{\min, \max}. \quad (8)$$

Under the bang–bang law (5), the system evolves as

$$\dot{x} = A(x - e_{1,2}). \quad (9)$$

Thus, under application of  $u_{\min}$  ( $u_{\max}$ ) the system rotates clockwise about  $e_1$  ( $e_2$ ) with an angular velocity  $\omega$ . Since switches must occur after no longer than  $\pi/\omega$  units of time, the switching curve can be constructed in the state space as follows (see Fig. 2). Beginning from  $x_r$ , two possible state trajectories are described by solving (9) backwards in time for  $\pi/\omega$  units of time, yielding the curves  $A_1x_r$  and  $B_1x_r$ . The segment  $B_2A_1$  is obtained by rotating  $B_1x_r$  about  $e_1$  by an angle  $\pi$  and scaling it by  $\exp[\frac{a_1\pi}{2\omega}]$ . Similarly the segment  $A_2B_1$  is obtained by rotating  $A_1x_r$  about  $e_2$  and scaling it by the same amount. This procedure is then repeated.

If the target point is equal to either of the points  $e_{1,2}$ , then there is no time-optimal solution as one of the rotation centers is also the target point; under application of the corresponding control

value the system will spiral in to the target in infinite time. For the remainder of this paper, then, we explicitly exclude  $e_{1,2}$  as target points.

This constructive procedure describes the switching curve but does not allow one to easily calculate the number of switches and switching times.

### 3. A pair of affine mappings

The normal coordinates are defined such that the final state trajectory under each control extreme is mapped to a logarithmic spiral. The coordinate transformation is achieved using one of two mappings. To construct them consider again (2) with a target point  $x_r$ . Shift the target point to the origin by defining  $\hat{x} = x - x_r$ . The dynamics are then

$$\dot{\hat{x}} = A\hat{x} + Ax_r + Bu.$$

Let  $\Phi(t, \tau)$  denote the state transition matrix of the system,  $\hat{x}_s$  a state on the final state trajectory, and  $t_s \geq 0$  the time to go from  $\hat{x}_s$  to the origin (or, equivalently, to  $x_r$  in the unshifted coordinates). Under an optimal control law, the evolution of the system from  $\hat{x}_s$  to the origin is given by the variation of constants formula to be

$$0 = \Phi(t_s, 0)\hat{x}_s + \int_0^{t_s} \Phi(t_s, \tau)(Ax_r + Bu)d\tau. \quad (10)$$

Pre-multiplying both sides of (10) by  $\Phi(0, t_s)$  and using  $\hat{x}_s = x_s - x_r$ , we obtain

$$x_s = x_r - \int_0^{t_s} \Phi(0, \tau)(Ax_r + Bu)d\tau. \quad (11)$$

Define the complex matrix

$$P = \begin{bmatrix} 1 & 1 \\ \lambda_1 & \lambda_2 \end{bmatrix}, \quad (12)$$

where  $\lambda_{1,2}$  are the eigenvalues of the system. Then

$$\int_0^{t_s} \Phi(0, \tau)d\tau = P \begin{bmatrix} \frac{(1 - e^{-\lambda_1 t_s})}{\lambda_1} & 0 \\ 0 & \frac{(1 - e^{-\lambda_2 t_s})}{\lambda_2} \end{bmatrix} P^{-1}. \quad (13)$$

Define variables  $v, z, m, n$  as:

$$Ax_r + Bu_{\min} = [m \ n]^T, \quad (14a)$$

$$Ax_r + Bu_{\max} = [v \ z]^T. \quad (14b)$$

Since the points  $e_{1,2}$  defined in (8) are excluded as target points, it cannot be that all the vectors in (14) are zero. The two branches of the final state trajectory, denoted  $x_{\min, \max}$ , can then be described in terms of  $t_s$  and  $x_r$  by substituting (3), (12) and (13) into (11). Carrying out some routine but tedious calculations yields

$$x_{\min, \max}(t_s) = A_{\min, \max} \begin{bmatrix} X(t_s) \\ Y(t_s) \end{bmatrix} + B_{\min, \max} \quad (15)$$

where

$$R(t) = e^{\frac{a_1}{2}t}, \quad (16a)$$

$$X(t) = R(t) \cos(\omega t), \quad Y(t) = R(t) \sin(\omega t), \quad (16b)$$

$$A_{\min} = \begin{bmatrix} -\frac{a_1 m + n}{a_2} & -\frac{m(4\omega^2 - a_1^2) - 2a_1 n}{4a_2 \omega} \\ m & -\frac{a_1 m + 2n}{2\omega} \end{bmatrix}, \quad (16c)$$

$$B_{\min} = x_r + \begin{bmatrix} \frac{a_1 m + n}{a_2} - m \end{bmatrix}^T, \quad (16d)$$

$$A_{\max} = \begin{bmatrix} -\frac{a_1 v + z}{a_2} & -\frac{v(4\omega^2 - a_1^2) - 2a_1 z}{4a_2 \omega} \\ v & -\frac{a_1 v + 2z}{2\omega} \end{bmatrix}, \quad (16e)$$

$$B_{\max} = x_r + \begin{bmatrix} \frac{a_1 v + z}{a_2} - v \end{bmatrix}^T. \quad (16f)$$

The relations in (15) give the final state trajectory in terms of the time to go and define the affine mappings,

$$M_{\min, \max}^+ : \mathbb{R}^2 \rightarrow \mathbb{R}^2, \quad \begin{bmatrix} X \\ Y \end{bmatrix} \mapsto \begin{bmatrix} x_1 \\ x_2 \end{bmatrix} = A_{\min, \max} \begin{bmatrix} X \\ Y \end{bmatrix} + B_{\min, \max}. \quad (17)$$

Note that there is a small abuse of notation here in reusing  $(X, Y)$  both as the curves in (16) and as the coordinates under the mapping  $M_{\min}^+$  or  $M_{\max}^+$ . The following lemma establishes the invertibility of the mappings.

**Lemma 1.** Consider (2) satisfying (4). If the target state  $x_r \neq e_{1,2}$ , then  $M_{\min}^+$  and  $M_{\max}^+$  are invertible mappings with inverses  $M_{\min}^-$  and  $M_{\max}^-$  given by

$$M_{\min, \max}^- : \mathbb{R}^2 \rightarrow \mathbb{R}^2, \quad \begin{bmatrix} x_1 \\ x_2 \end{bmatrix} \mapsto \begin{bmatrix} X \\ Y \end{bmatrix} = A_{\min, \max}^{-1} \left( \begin{bmatrix} x_1 \\ x_2 \end{bmatrix} - B_{\min, \max} \right). \quad (18)$$

**Proof.** To show  $M_{\min}^+$  is invertible, we need only show that  $A_{\min}$  is invertible. Its determinant is

$$\det(A_{\min}) = \frac{(n - \lambda_1 m)(n - \lambda_2 m)}{a_2 \omega}. \quad (19)$$

By assumption,  $x_r \neq e_1$  and so  $Ax_r + Bu_{\min} \neq 0$ . From (14), then, at least one of  $m$  and  $n$  is non-zero. Then, from (19),  $\det(A_{\min})$  is non-zero and thus  $A_{\min}$  is nonsingular. A similar argument holds for  $M_{\max}^+$ .  $\square$

For space reasons, in the remainder of this paper we arbitrarily focus on  $M_{\min}^+$ . Similar results hold for  $M_{\max}^+$ .

We call the variables  $(X, Y)$  the *normal coordinates*. The mapping  $M_{\min}^-$  transforms the original state variables into the normal coordinates according to (18). It is straightforward to show that

$$[\dot{X}(t) \ \dot{Y}(t)]^T = A_n [X(t) \ Y(t)]^T + B_n u + C_n$$

where

$$A_n = A_{\min}^{-1} A A_{\min} = \begin{bmatrix} -\frac{a_1}{2} & \omega \\ -\omega & -\frac{a_1}{2} \end{bmatrix},$$

$$B_n = A_{\min}^{-1} B, \quad C_n = A_{\min}^{-1} A B_{\min}.$$

A simple calculation shows that  $B_n u_{\min} + C_n = 0$ . As seen from (16),  $M_{\min}^-$  transforms the optimal final state trajectory corresponding to  $u_{\min}$  to a logarithmic spiral in the normal coordinates. The following theorem establishes that the optimal final state trajectory corresponding to  $u_{\max}$  is similar to the one corresponding to  $u_{\min}$  (in a geometric sense).

**Theorem 1.** If  $x_r \neq e_{1,2}$ , then the two final state trajectories corresponding to  $u_{\min}$  and  $u_{\max}$  under the map  $M_{\min}^{-1}$  are related by a rotation, dilation, and translation. Further, the angle of rotation between the two is given by

$$\tan \theta = \left( \frac{2\omega(mz - nv)}{m(2a_2 v + a_1 z) + n(a_1 v + 2z)} \right), \quad (20)$$

the dilation is

$$\eta = \sqrt{\frac{(\lambda_1 v - z)(\lambda_2 v - z)}{(\lambda_1 m - n)(\lambda_2 m - n)}}, \quad (21)$$

and the translation is

$$v = A_{\min}^{-1} (B_{\max} - B_{\min}). \quad (22)$$

**Proof.** The final state trajectory corresponding to  $u_{\min}$  under the map  $M_{\min}^-$  is the spiral curve (16). Consider now the final state trajectory corresponding to  $u_{\max}$ , given by (15). Transforming this with  $M_{\min}^-$  yields

$$\begin{bmatrix} X_{\max} \\ Y_{\max} \end{bmatrix} = A_{\min}^{-1} A_{\max} \begin{bmatrix} X_{\min} \\ Y_{\min} \end{bmatrix} + A_{\min}^{-1} (B_{\max} - B_{\min}) \quad (23)$$

where we have denoted the final state trajectory under the  $M_{\min}^-$  mapping as  $[X_{\min} \ Y_{\min}]^T$ . Defining  $v$  as in (22) establishes the translation term. A simple calculation shows that  $A_{\min}^{-1} A_{\max}$  is given by

$$\begin{bmatrix} \frac{(a_1 n + 2a_2 m)v + (a_1 m + 2n)z}{2(\lambda_1 m - n)(\lambda_2 m - n)} & \frac{\omega(nv - mz)}{2(\lambda_1 m - n)(\lambda_2 m - n)} \\ -\frac{\omega(nv - mz)}{2(\lambda_1 m - n)(\lambda_2 m - n)} & \frac{(\lambda_1 m - n)(\lambda_2 m - n)}{(a_1 n + 2a_2 m)v + (a_1 m + 2n)z} \end{bmatrix}.$$

Since the diagonal terms in this matrix are equal while the skew-diagonal terms differ only by a sign, this matrix represents a rotation and a dilation.

To calculate the rotation angle and dilation factor, consider Fig. 3. In the original coordinates, under  $u_{\min}$  ( $u_{\max}$ ), the system rotates about  $B_{\min}$  ( $B_{\max}$ ), proceeding to the target  $x_r$ . Under the map  $M_{\min}^-$ ,  $x_r$  is mapped to the point  $[1 \ 0]^T$  (denoted  $O$  in Fig. 3), the final trajectory under  $u_{\min}$  is mapped to the standard spiral curve defined in (16), the point  $B_{\min}$  is mapped to the origin (denoted  $C_0$  in the figure), and the point  $B_{\max}$  is mapped to  $C_1$ . Applying  $M_{\min}^-$  to  $B_{\max}$  shows that

$$C_1 = \begin{bmatrix} 1 - \frac{m(2a_2 v + a_1 z) + n(a_1 v + 2z)}{2(u_1 m - n)(u_2 m - n)} \\ \frac{\omega(nv - mz)}{(u_1 m - n)(u_2 m - n)} \end{bmatrix}. \quad (24)$$

$\theta$  is the angle from  $C_0$  to  $C_1$  while  $\eta$  is the ratio of the lengths of the line segments  $\|C_1 O\|/\|C_0 O\|$ . Using (24), these are given by (20) and (21), respectively.  $\square$

#### 4. The switching curve in normal coordinates

The properties of  $M_{\min}^-$  allow for a general method for the construction of the switching curve in the normal coordinates. For the remainder of this paper, we consider only holdable equilibrium target states.

**Lemma 2.** For holdable equilibrium target states, the relative orientation angle of the two final state trajectories in the normal coordinates is  $\theta = \pi$ .

**Proof.** From Definition 1 and the assumption that  $x_r \neq e_{1,2}$ , there exists a  $u_o \in (u_{\min}, u_{\max})$  such that  $Ax_r + Bu_o = 0$ . Using this in (14) yields

$$\begin{aligned} v &= b_1(u_{\max} - u_o), & z &= (b_2 - a_1 b_1)(u_{\max} - u_o), \\ m &= b_1(u_{\min} - u_o), & n &= (b_2 - a_1 b_1)(u_{\min} - u_o). \end{aligned}$$

From this it follows that  $mz - nv = 0$ . Using this in (20) yields  $\theta = \tan^{-1}(0)$  and thus  $\theta = 0$  or  $\pi$ . As stated in the proof of

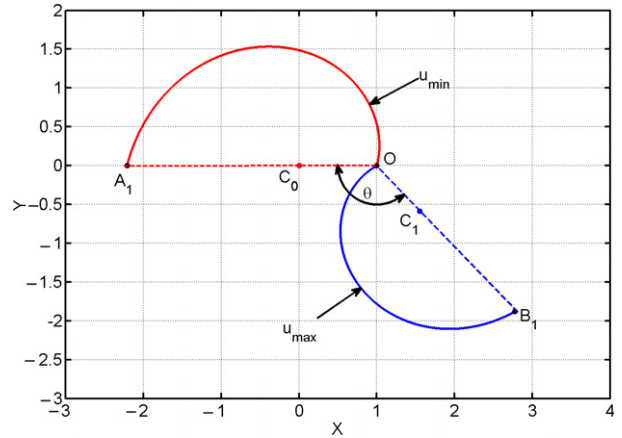


**Fig. 3.** The two final state trajectories under  $u_{\min}$  (red) and  $u_{\max}$  (blue) in the normal coordinates (under  $M_{\min}^-$ ). The trajectory under  $u_{\min}$  is mapped to a logarithmic spiral passing through the point  $O = [1 \ 0]^T$  (the target point), and rotating about the origin ( $C_0$ ). The trajectory under  $u_{\max}$  is also a spiral curve passing through  $O$  but rotating about  $C_1$ . (For interpretation of the references to colour in this figure legend, the reader is referred to the web version of this article.)

**Theorem 1,** the rotation centers  $e_{1,2}$  are mapped to  $C_0$  and  $C_1$ . For a holdable equilibrium point, these are

$$C_0 = [0 \ 0]^T, \quad C_1 = [1 - q \ 0]^T$$

where

$$q = \frac{m(2a_2 v + a_1 z) + n(a_1 v + 2z)}{2(n^2 + a_1 m n + a_2 m^2)}.$$

The inner product between the vectors  $C_0 O$  and  $C_1 O$  (see Fig. 3) is given by  $q$ . Therefore  $\theta = \pi$  if  $q < 0$ . Plugging  $m$ ,  $n$ ,  $v$ , and  $z$  into the definition of  $q$  yields

$$q = -2 \left[ \omega^2 b_1^2 + \left( \frac{a_1 b_1}{2} + b_2 \right)^2 \right] (u_o - u_{\min})(u_{\max} - u_o).$$

For a holdable equilibrium point,  $u_{\min} < u_o < u_{\max}$  and therefore  $q < 0$ . Thus,  $\theta = \pi$ .  $\square$

Due to (7), the final switching curve is in general only a portion of the final state trajectory. The next theorem establishes that for holdable equilibrium target states the final switching curve is the entire final state trajectory.

**Theorem 2.** For a holdable equilibrium target state, if the switching curve exists, then the final switching curve is the entire final state trajectory for both  $u_{\min}$  and  $u_{\max}$ .

**Proof.** From the definition of a holdable target state, we have that  $Ax_r + Bu_o = 0$  for some  $u_o \in (u_{\min}, u_{\max})$ . Adding and subtracting either  $Bu_{\min}$  or  $Bu_{\max}$  to this and rearranging yields the two results

$$Ax_r + Bu_{\min, \max} = B(u_{\min, \max} - u_o).$$

Thus the vectors  $Ax_r + Bu_{\min, \max}$  lie along the line in the costate space defined by  $Bu_{\min, \max}$  (see Fig. 1), perpendicular to the switching line. Since they have opposite direction, the boundary condition (7) is satisfied for any  $\psi(t_f)$  in the half-plane corresponding to either  $u_{\min}$  or  $u_{\max}$ . Therefore, the final switching curve can be extended backwards for  $\pi/\omega$  units of time, corresponding to the entire final state trajectory.  $\square$

With these results, it follows that the switching curve in normal coordinates is made of segments of logarithmic spirals. An example switching curve is shown in Fig. 4. The two final portions corresponding to  $u_{\min}$  (red,  $A_1 O$ ) and  $u_{\max}$  (blue,  $B_1 O$ ) both terminate at the target state  $O$ . The component of the switching curve  $B_2 A_1$  is

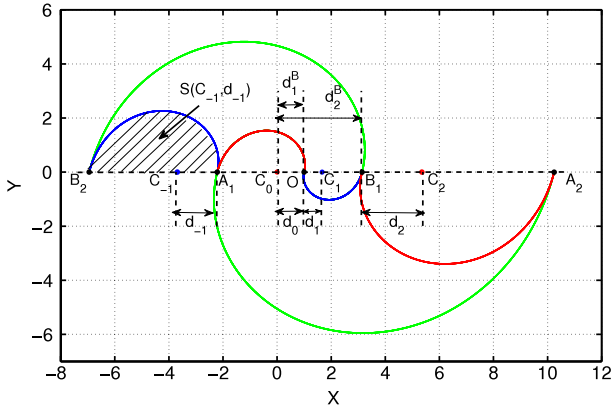


Fig. 4. An example switching curve for a holdable equilibrium target state in normal coordinates.

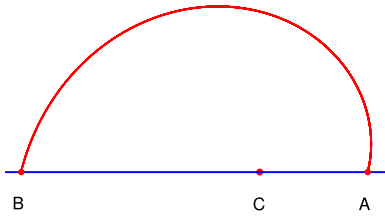


Fig. 5. A logarithmic spiral over  $\pi$  radians with center  $C$ , size  $\|CA\|$  and scaling factor  $\|CB\|/\|CA\|$ .

obtained by rotating the curve  $B_1O$  about the point  $C_0$  by  $\pi$  radians and scaling it by a factor of  $\exp[\frac{a_1\pi}{2\omega}]$ . Similarly, the component of the switching curve  $A_2B_1$  is obtained by rotating  $A_1O$  about the point  $C_1$  by  $\pi$  radians and scaling it by the same factor. The next portion of the curve is generated by rotating  $A_2B_1$  about  $C_0$  and  $B_2A_1$  about  $C_1$  and scaling both the factor  $\exp[\frac{a_1\pi}{2\omega}]$ . Repeating this process yields the entire switching curve.

The construction procedure above gives rise to three types of spiral curve segments defining the time-optimal solution. The first (in red in Fig. 4) corresponds to switches along trajectories that end with the control  $u_{\min}$ , the second (in blue) corresponds to switches along trajectories that end with  $u_{\max}$  and the third (in green) denotes boundaries separating regions of these trajectories. Any trajectory that begins in the same region has the same sequence of controls and number of switches.

## 5. Calculating the number of switches and the switching times

Consider a standard logarithmic spiral that begins on the  $x$ -axis and rotates for  $\pi$  radians (Fig. 5). This curve can be described by its center  $C$  defined by the point about which the curve spirals, its size  $d$  defined by the length  $\|CA\|$ , and its scaling factor  $\gamma$  defined by the ratio

$$\gamma = \|CB\|/\|CA\|. \quad (25)$$

Consider the switching curve in Fig. 4. Denote the rotation centers for each segment of the switching curve for a holdable equilibrium target point as  $C_k$ ,  $k = \dots, -2, -1, 0, 1, 2, \dots$ , with  $k < 0$  for those segments of the switching curve to the left of the origin,  $k = 0$  for the origin, and  $k > 0$  for those to the right of the origin. Similarly, let  $d_k$ ,  $k = \dots, -2, -1, 0, 1, 2, \dots$ , denote the size of each spiral segment of the switching curve. All of the spirals have the same scaling factor, given by

$$\gamma = e^{\frac{a_1\pi}{2\omega}}. \quad (26)$$

Define  $c = \|C_0 - C_1\|$  as the distance between the rotation centers.

From Fig. 4, it is clear that the boundary spirals separate the space into regions. States in one region have the same number of switches. Determining the number of switches is equivalent to finding which region the initial point sits in. The following lemma establishes that we need only consider initial points in the upper closed-half-plane.

**Lemma 3.** Let  $x_0$  be any initial state in the original coordinates and define the two points  $p_{\min}$  and  $p_{\max}$  by

$$p_{\min, \max} = [X_{\min, \max}^o \quad Y_{\min, \max}^o]^T = M_{\min, \max}^- x_0.$$

Then one of  $p_{\min}$ ,  $p_{\max}$  is in the upper closed-half-plane and the other is in the lower closed-half-plane.

**Proof.** From the definition of  $M_{\max}^-$  in (18) we have that

$$p_{\max} = A_{\max}^{-1} (x_0 - B_{\max}).$$

Rearranging yields  $x_0 = A_{\max} p_{\max} + B_{\max}$ . Then, from the definition of  $M_{\min}^-$  in (18),

$$\begin{aligned} p_{\min} &= A_{\min}^{-1} (x_0 - B_{\min}) \\ &= A_{\min}^{-1} (A_{\max} p_{\max} + B_{\max} - B_{\min}). \end{aligned}$$

This is the same as (23). Thus the two points are related by a rotation  $\theta$ , a dilation  $\eta$ , and a translation  $v$  along the  $X$ -axis. From Lemma 2,  $\theta = \pi$ , proving the lemma.  $\square$

Consider now the boundary spirals in the upper half-plane. From Fig. 4, the first is the final switching curve  $A_1O$ , the second is the curve  $B_1B_2$  and so on. Index these curves with  $k = 1, 2, 3, \dots$ . All have their center at the origin  $C_0$  and scaling factor  $\gamma$ . Denote the size of the  $k$ th as  $d_k^B$ . The following lemma establishes these sizes.

**Lemma 4.** Let  $d_0^B = 0$  and  $d_1^B = 1$ . Then the sizes of the boundary spiral segments are given by

$$d_{2k}^B = \frac{((c-1)\gamma + 1)\gamma^{2k-1} - c}{\gamma - 1}, \quad (27a)$$

$$d_{2k+1}^B = 1 + \frac{(\gamma^{2k} - 1)(\gamma + c - 1)}{\gamma - 1}, \quad (27b)$$

for  $k = 1, 2, 3, \dots$

**Proof.** The sizes can be expressed inductively as

$$d_{2k+3}^B - d_{2k+2}^B = (1 + \gamma)\gamma^{2k+1}, \quad (28a)$$

$$d_{2k+2}^B - d_{2k+1}^B = (c-1)(1 + \gamma)\gamma^{2k}, \quad (28b)$$

for  $k = 0, 1, 2, \dots$ . Combining these two yields

$$d_{2k+3}^B - d_{2k+1}^B = (1 + \gamma)\gamma^{2k+1} + (c-1)(1 + \gamma)\gamma^{2k}.$$

Summing both sides of this equation from 0 to  $k$  yields

$$d_{2k+3}^B - d_1^B = \sum_{i=0}^k \{(1 + \gamma)\gamma^{2i+1} + (c-1)(1 + \gamma)\gamma^{2i}\}.$$

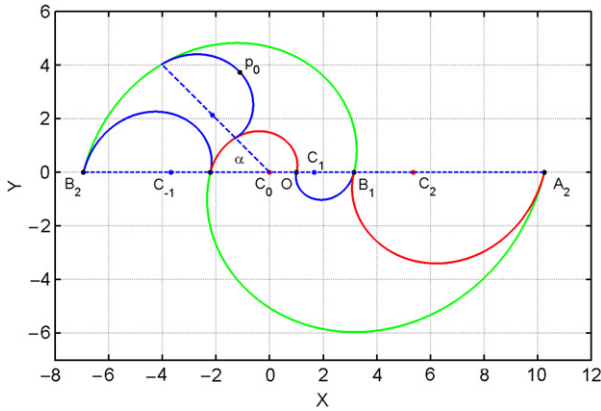
Carrying out the sum and using  $d_1^B = 1$  yields

$$d_{2k+3}^B = 1 + (\gamma + c - 1) \frac{\gamma^{2k+2} - 1}{\gamma - 1}. \quad (29)$$

Rearranging (28) for  $d_{2k+2}^B$  and replacing in (29) yields

$$d_{2k+2}^B = \frac{((c-1)\gamma + 1)\gamma^{2k+1} - c}{\gamma - 1}.$$

Reassigning  $2k$  for  $2k+2$  results in the form in (27a) and doing so similarly in (29) yields (27b).  $\square$

Fig. 6. A starting angle for a given initial condition  $p_0$ .

Note that for an unstable system,  $a_1 < 0$  and thus, from (26),  $0 < \gamma < 1$ . As a result,

$$\lim_{k \rightarrow \infty} d_{2k}^B = \lim_{k \rightarrow \infty} d_{2k+1}^B = c(1 - \gamma)^{-1}.$$

This implies that the boundary trajectories converge to a spiral segment of size  $\frac{c}{1-\gamma}$ . Only initial conditions inside this boundary can be driven to the target state due to the limitations on the magnitude of the control signal.

**Lemma 5.** The centers and sizes of the spiral curve segments of the switching curve are given by

$$C_k = \begin{cases} \frac{\gamma d_k^B + d_{k+1}^B}{1 + \gamma}, & k = 1, 2, 3, \dots, \\ 0, & k = 0, \\ \frac{\gamma(\gamma d_{-k}^B + d_{1-k}^B)}{1 + \gamma}, & k = -1, -2, -3, \dots, \end{cases} \quad (30)$$

and

$$d_k = \begin{cases} \frac{d_{k+1}^B - d_k^B}{1 + \gamma}, & k = 1, 2, 3, \dots, \\ 1, & k = 0, \\ \frac{\gamma(d_{1-k}^B - d_{-k}^B)}{1 + \gamma}, & k = -1, -2, -3, \dots \end{cases} \quad (31)$$

**Proof.** By construction (see Fig. 4), for  $k > 0$ , the rotation center  $C_k$  lies on the positive X-axis between  $d_k^B$  and  $d_{k+1}^B$ . Using this in (25) yields

$$\gamma = \frac{d_{k+1}^B - C_k}{C_k - d_k^B}.$$

For  $k < 0$ ,  $C_k$  is on the negative X-axis at a distance between  $\gamma d_{-k}^B$  and  $\gamma d_{1-k}^B$ . Using this in (25) yields

$$\gamma = \frac{C_k - \gamma d_{1-k}^B}{\gamma d_{-k}^B - C_k}.$$

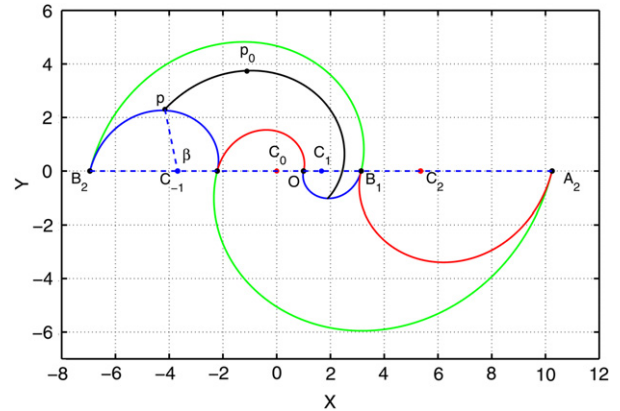
Rearranging these two equations yields (30). Consider now the  $k$ th spiral segment,  $k > 0$ . By construction of the boundary trajectories, the distance between the two endpoints of the segment on the X-axis is  $d_{k+1}^B - d_k^B$ . Using (25), it is also given by  $d_k + \gamma d_k$ . Thus

$$d_k + \gamma d_k = d_{k+1}^B - d_k^B.$$

Equating the distances analogously for  $k < 0$  yields

$$d_k + \gamma d_k = \gamma d_{1-k}^B - \gamma d_{-k}^B.$$

Rearranging these two yields (31).  $\square$

Fig. 7. A shooting angle for a given initial condition  $p_0$ .

### 5.1. Calculating the number of switches

Consider the  $k$ th switching curve section,  $k < 0$ . Let  $S(C_k, d_k)$  denote the region formed by the X-axis and this section (Fig. 4). The number of switches,  $K$ , to drive an initial state to the target state and the initial control value can be calculated by the following algorithm.

**Algorithm (Number of Switches).**

0. Map the initial state  $x_0$  to  $p_{\min}$  and  $p_{\max}$  using  $M_{\min}^-$  and  $M_{\max}^-$  respectively. Select one that lies on or above the X-axis. Denote the selected point as  $p_0$ .

1. Find the integer  $k \geq 0$  such that

$$d_k^B < \|p_0\| e^{-\frac{\alpha_1 \theta}{2\omega}} \leq d_{k+1}^B$$

where  $\theta$  is the angle from the X-axis to  $p_0$  (with counter-clockwise being positive).

2. If  $p_0 \in S(C_{-k}, d_{-k})$  the number of switches is  $K = k + 1$  and the initial control value is  $u_{\max}$  ( $u_{\min}$ ) if  $M_{\min}^-$  ( $M_{\max}^-$ ) was used. Otherwise  $K = k$  and the initial control value is  $u_{\min}$  ( $u_{\max}$ ) if  $M_{\min}^-$  ( $M_{\max}^-$ ) was used.

### 5.2. Calculating the switching times

In Section 2.1 it was shown that the duration between intermediate switches is  $\pi/\omega$  units of time while those of the first and last are determined by the initial and final direction of the costate. To calculate these intervals in the normal coordinates, we first define two angles as follows.

**Definition 2.** Consider an initial condition  $p_0$  above the X-axis as illustrated in Fig. 6. If  $p_0 \in S(C_{-k}, d_{-k})$  then the *starting angle*  $\alpha$  is the angle by which the switching curve segment is rotated counter-clockwise about  $C_1$  (so that  $\alpha$  is positive) until it intersects with  $p_0$ . Otherwise,  $\alpha$  is the angle by which the switching curve segment is rotated clockwise about  $C_0$  until it intersects with  $p_0$ .

The time  $\alpha/\omega$  represents the duration it would have taken the system to proceed either from the previous switch to the initial condition (if  $\alpha$  is negative) or from the initial condition to the next switch (if  $\alpha$  is positive).

**Definition 3.** Consider an initial condition  $p_0$  above the X-axis (see Fig. 7). If  $p_0 \in S(C_{-k}, d_{-k})$  evolve the system forward in time along the optimal trajectory until the switching curve is intersected, else evolve backward in time. Denote the intersection as  $p$ . The *shooting angle*  $\beta$  is the angle between the line  $p-C_{-k}$  and the X-axis.

By similarity of the switching curve segments,  $p$  represents where the system will intersect the final switching curve. Thus the final interval will be  $\beta/\omega$  units of time. Using these definitions, the switching times and the total transition time can be calculated according as follows.

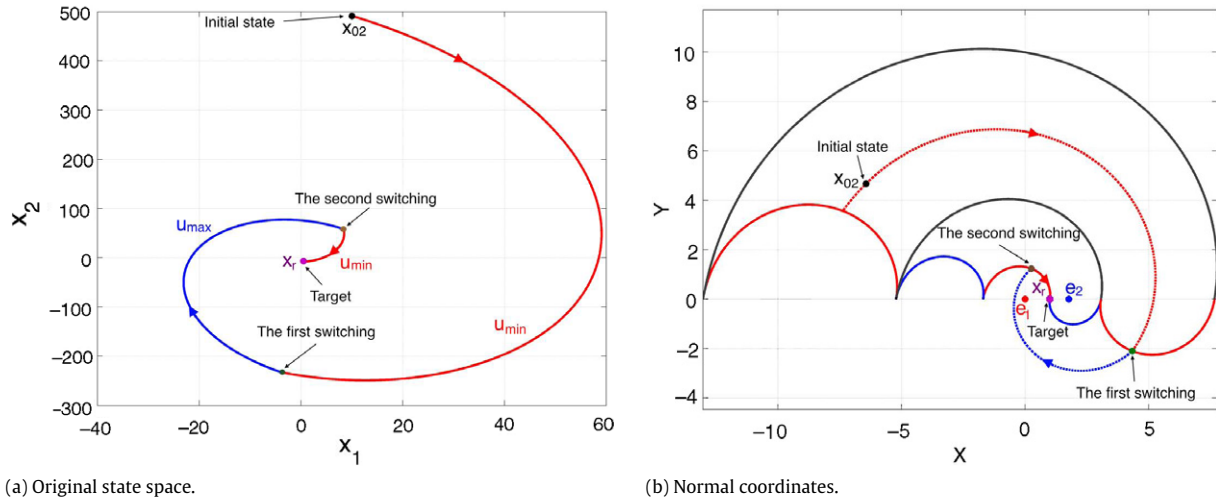


Fig. 8. Switching curves, initial conditions, and optimal trajectories from  $x_0 = [10.0401 \ 491.0869]^T$  in both the original and the normal coordinates.

#### Algorithm (Switching Times).

0. Map the initial state  $x_0$  to  $p_{\min}$  and  $p_{\max}$  using  $M_{\min}^-$  and  $M_{\max}^-$  respectively. Select one that lies on or above the  $X$ -axis. Denote the selected point as  $p_0$ .
1. Calculate (numerically) the starting angle  $\alpha$  and the shooting angle  $\beta$ .
2. Calculate the total number of switches  $K$ .
3. The time of the first switch is

$$t_1 = \begin{cases} \frac{\pi + \alpha}{\omega}, & \alpha < 0, \\ \frac{\alpha}{\omega}, & \alpha \geq 0. \end{cases} \quad (32)$$

The times of the intermediate switches are

$$t_k = t_1 + \frac{\pi}{\omega}(k-1), \quad k = 2, 3, \dots, K-1. \quad (33)$$

The total time to make the transfer is

$$T_s = t_1 + \frac{(K-1)\pi + \beta}{\omega}. \quad (34)$$

#### 5.3. A feedback control law

The switching structure in the normal coordinates allows for a simple feedback control law to generate an optimal trajectory. Given the current state  $x(t)$ , map it to the normal coordinates using either  $M_{\min}^-$  or  $M_{\max}^-$  such that the mapped point lies on or above the  $X$ -axis; denote this point  $p$ . Determine the integer  $k \geq 0$  such that

$$d_k^B < \|p\| e^{-\frac{\alpha_1 \theta}{2\omega}} \leq d_{k+1}^B.$$

Then an optimal feedback control law is as follows. If  $M_{\min}^-$  was used then

$$u^*(p) = \begin{cases} u_{\max}, & p \in S(C_{-k}, d_{-k}), \\ u_{\min}, & \text{else,} \end{cases} \quad (35)$$

while if  $M_{\max}^-$  was used then

$$u^*(p) = \begin{cases} u_{\min}, & p \in S(C_{-k}, d_{-k}), \\ u_{\max}, & \text{else.} \end{cases} \quad (36)$$

#### 6. An example

To illustrate the algorithm in this paper, consider a second order system in observable canonical form given by

$$\dot{x} = \begin{bmatrix} 0 & 1 \\ -36 & -2 \end{bmatrix} x + \begin{bmatrix} 50 \\ 36 \end{bmatrix} u \triangleq Ax + Bu. \quad (37)$$

The eigenvalues are  $\lambda_{1,2} = -1 \pm 5.92i$ . Let the control be restricted to  $u \in [-1, 1]$  and let the target state be  $x_r = [0.5 \ -6.6176]^T$ . This target is a holdable equilibrium point since  $Ax + Bu_0 = 0$  is satisfied for  $u_0 = 0.13235$ . We consider the initial condition  $x_0 = [10.0401 \ 491.0869]^T$ . This point is plotted in both the original and normal coordinates in Fig. 8(a,b). From the position of the initial condition in the normal coordinates, it is clear that there are two switches and that the initial control value is  $-1$ . The initial and shooting angles were  $169.83^\circ$  and  $78.310^\circ$ , respectively. From these, the first switching time was found to be  $0.50103$  s and the second at  $\pi/\omega = 0.53103$  s later (i.e. at  $1.03206$  s). The total transition time was  $1.26319$  s.

#### 7. Conclusions and future work

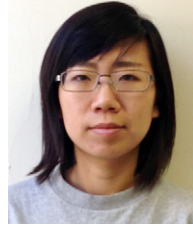
In this work we proposed a new approach to construct the switching curve for the time-optimal control of a second-order LTI system. Using one of a pair of affine mappings, the system is transformed into normal coordinates in which the switching pattern is given by similar logarithmic spirals. The construction allows for simple algorithms to determine the number of switches and the total switching time required to transfer the system from a given initial condition to the target state as well as the time of each of the switches in the sequence.

The results are limited to holdable equilibrium points since for other target points, the final switching curve may no longer correspond to the entire final state trajectory. In addition, it is well known that the bang–bang control law is sensitive to both external disturbances and modeling uncertainty. Despite this concern, however, the ability to know *a priori* the total switching time can be useful in problems where the system needs to move through a sequence of points. Optimizing the entire transit time can be done by knowing the transit time between any pair of points and then solving the corresponding “traveling salesman” problem.

#### References

- Andersson, S.B., & Pao, L.Y. (2012). Non-raster sampling in atomic force microscopy: a compressed sensing approach. In *Proceedings of the american control conference* (pp. 2485–2490).
- Iamratanakul, D., Jordan, B., Leang, K. K., & Devasia, S. (2008). Optimal output transitions for dual-stage systems. *IEEE Transactions on Control Systems Technology*, 16(5), 869–881.
- Khaneja, N., Brockett, R. W., & Glaser, S. J. (2001). Time optimal control in spin systems. *Physical Review A*, 63, 032308.
- Khaneja, N., Reiss, T., Kehlet, C., Schulte-Herbrüggen, T., & Glaser, S. J. (2005). Optimal control of coupled spin dynamics: design of nmr pulse sequences by gradient ascent algorithms. *Journal of Magnetic Resonance*, 172(2), 296–305.

- La-orpacharapan, C., & Pao, L. Y. (2004). Shaped time-optimal feedback control for disk-drive systems with back-electromotive force. *IEEE Transactions on Magnetics*, 40(1), 85–96.
- McCormick, J., & Horowitz, R. (1991). Time optimal seek trajectories for a dual stage optical disk drive actuator. *Journal of Dynamic Systems, Measurement, and Control*, 113(3), 534–536.
- Pontryagin, L. S., Boltyanskii, V. G., Gamkrelidze, R. V., & Mishchenko, E. F. (1962). *The mathematical theory of time optimal processes*. Interscience.
- Shen, Z., & Andersson, S. B. (2011). Tracking nanometer-scale fluorescent particles in two-dimensions with a confocal microscope. *IEEE Transactions on Control Systems Technology*, 19(5), 1269–1278.



**Peng Huang** was born in Jilin, China, in 1983. She received her B.S. in electrical engineering and power systems from Tsinghua University, Beijing, China, in 2006 and her M.S. of electrical engineering from the Chinese Academy of Sciences, Beijing, China, in 2009. She is currently a Ph.D. candidate in mechanical engineering, Boston University. Her research interests include high speed atomic force microscopy, and control and modeling in nanopositioning systems.



**Zhaolong Shen** received B.E. and M.E. degrees in mechanical and electronic engineering (University of Science and Technology of China, 2004 and 2007), and a Ph.D. degree in mechanical engineering (Boston University, 2011). He is currently a postdoctoral research associate (University of Maryland, College Park). His research interests include biomedical imaging, magnetic drug targeting, control of micro/nano-scale systems, and design and analysis of networked control systems.



**Sean B. Andersson** received a B.S. in engineering and applied physics (Cornell University, 1994), an M.S. in mechanical engineering (Stanford University, 1995), and a Ph.D. in electrical and computer engineering (University of Maryland, College Park, 2003). He has worked at AlliedSignal Aerospace and Aerovironment, Inc. and is currently an Associate Professor of mechanical engineering and of systems engineering with Boston University. His research interests include systems and control theory with applications in scanning probe microscopy, dynamics in molecular systems, and robotics.